5-1-2015

Estimating forest structure in a tropical forest using field measurements, a synthetic model and discrete return lidar data

Michael W. Palace
University of New Hampshire, Durham, michael.palace@unh.edu

Franklin B. Sullivan
University of New Hampshire, Durham, Franklin.Sullivan@unh.edu

Mark J. Ducey
University of New Hampshire, Durham, mark.ducey@unh.edu

Robert N. Treuhaft
California Institute of Technology

Christina Herrick
University of New Hampshire, Durham, christina.herrick@unh.edu

See next page for additional authors

Follow this and additional works at: https://scholars.unh.edu/faculty_pubs

Recommended Citation

Authors

Michael W. Palace, Franklin B. Sullivan, Mark J. Ducey, Robert N. Treuhaft, Christina Herrick, Julia Z. Shimbo, and Jonas Mota-E Silva

Estimating forest structure in a tropical forest using field measurements, a synthetic model and discrete return lidar data

Michael W. Palace [a], Franklin B. Sullivan [a], Mark J. Ducey [b], Robert N. Treuhaft [c], Christina Herrick [a], Julia Z. Shimbo [d], Jonas Mota-E-Silva [e]

[a] Earth Systems Research Center, Institute for the Study of Earth, Oceans, and Space, University of New Hampshire, United States
[b] Department of Natural Resources and the Environment, James Hall, University of New Hampshire, United States
[c] Jet Propulsion Laboratory, California Institute of Technology, United States
[d] Universidade de Brasília, Instituto de Ciências Biológicas, Brazil
[e] Universidade de Brasília, Instituto de Geociências, Brazil

ABSTRACT

Tropical forests are huge reservoirs of terrestrial carbon and are experiencing rapid degradation and deforestation. Understanding forest structure proves vital in accurately estimating both forest biomass and also the natural disturbances and remote sensing is an essential method for quantification of forest properties and structure in the tropics. Our objective is to examine canopy vegetation profiles formulated from discrete return LIght Detection And Ranging (lidar) data and examine their usefulness in estimating forest structural parameters measured during a field campaign. We developed a modeling procedure that utilized hypothetical stand characteristics to examine lidar profiles. In essence, this is a simple method to further enhance shape characteristics from the lidar profile. In this paper we report the results comparing field data collected at La Selva, Costa Rica (10° 26′ N, 83° 59′ W) and forest structure and parameters calculated from vegetation height profiles and forest structural modeling. We developed multiple regression models for each measured forest biometric property using forward stepwise variable selection that used Bayesian information criteria (BIC) as selection criteria. Among measures of forest structure, ranging from tree lateral density, diameter at breast height, and crown geometry, we found strong relationships with lidar canopy vegetation profile parameters. Metrics developed from lidar that were indicators of height of canopy were not significant in estimating plot biomass (p-value $= 0.31$, $r^2 = 0.17$), but parameters from our synthetic forest model were found to be significant for estimating many of the forest structural properties, such as mean trunk diameter (p-value $= 0.004$, $r^2 = 0.51$) and tree density (p-value $= 0.002$, $r^2 = 0.43$). We were also able to develop a significant model relating lidar profiles to basal area (p-value $= 0.003$, $r^2 = 0.43$). Use of the full lidar profile provided additional avenues for the prediction of field based forest measure parameters. Our synthetic canopy model provides a novel method for examining lidar metrics by developing a look-up table of profiles that determine profile shape, depth, and height. We suggest that the use of metrics indicating canopy height derived from lidar are limited in understanding biomass in a forest with little variation across the landscape and that there are many parameters that may be gleaned by lidar data that inform on forest biometric properties.

© 2015 The Authors. Published by Elsevier Inc. This is an open access article under the CC BY-NC-ND license (http://creativecommons.org/licenses/by-nc-nd/4.0/).

1. Introduction

Tropical forests are huge reservoirs of terrestrial carbon and are experiencing rapid degradation and deforestation. REDD+ is a UN based initiative to retain forests and subsequent carbon through payment to maintain existing forested regions (http://www.un-redd.org). Understanding forest structure proves vital in accurately estimating both forest biomass and also the natural disturbances and regrowth important in REDD+ planning (Asner, 2011; Asner et al., 2013; Berenguer et al., 2014). Remote sensing proves an essential tool for quantifying forest properties and structure due to the vastness and remoteness of many forests in the tropics (Frolking et al., 2009).

Forests are complex ecosystems with diverse species assemblages, crown structures, size class distributions, and historical disturbances (Asner et al., 2002; Broadbent, Asner, Peña-Claros, Palace, & Soriano, 2008; Clark et al., 2001; Keller, Asner, Silva, Palace, 2004; McMichael et al., 2013, 2014; Palace et al., 2008). Tropical forests have been argued to be the most structurally diverse forests (Richards 1952; Whitmore, 1982). Forest structural components include canopy geometry and tree architecture, size distributions of trees, and species diversity (Hurtt et al., 2003; Spies, 1998). These structural properties of forests are closely linked with ecosystem functioning (Clark et al., 2001; Frolking et al., 2009; Spies, 1998). The dynamic processes of growth and disturbance are reflected in the structural components of forests,

such as tree trunk diameter size distributions and canopy profiles, defined as the vertical distribution of foliage (Rice et al., 2004; Shugart, Hopkins, Burgess, & Mortlock, 1980; Tansley, 1935; Unger, Homeier, & Leuschner, 2013). The structural complexity of forests makes monitoring, understanding, and forecasting carbon dynamics difficult (Frolking et al., 2009). In tropical forests, gap formation or the death of individual trees is considered the prime disturbance mechanism (Denslow, 1987; Espírito-Santo et al., 2014; Vitousek & Denslow, 1986).

Knowledge of the three dimensional canopy structure of tropical forests is important for understanding gap formation and dynamics, light penetration, and surface roughness; all potential parameters in ecological models that are demographic, physiological, or physical in nature (Aber, 1979a; Denslow, 1987; Hartshorn, 1980; Marthews, Burslem, Phillips, & Mullins, 2008; Monsi, Uchijima, & Oikawa, 1973; Schemske & Brokaw, 1981; Terborgh, 1985). Specific forest structural properties are more easily measured, such as trunk diameter, and are links to providing insight and understanding of other properties that are more difficult to measure, such as biomass (Chave, Riéra, & Dubois, 2001). In addition forest structure provides insight into ecological processes and forest dynamics. One structural aspect of forests, the vertical profile of canopy vegetation, contains information about foliage distribution, trunk size distribution, light penetration and availability for understory vegetation, and canopy geometry (MacArthur & MacArthur, 1961, Stark et al., 2012; Sullivan, Palace, Ducey, 2014). Equations that estimate canopy profiles have been developed that link the MacArthur and Horn (1969) framework to broader statistical methodology, improving efficiency, flexibility, and the ability to incorporate auxiliary information (Aber, 1979a, 1979b; Maynard et al. 2013; Ni-Mester, Jupp, & Dubayah, 2001). LIght Detection And Ranging (lidar) data has been tested for efficacy within the forests (Chambers et al., 2007; DeFries, 2008, Stark et al., 2012; Sullivan et al., 2014). Lidar remote sensing has potential to measure properties of the forest through and below the top of the canopy, thus providing an additional dimension to structure studies (Hilker et al., 2014; Jensen, Humes, Vierling, & Hudak, 2008; Tang et al., 2012; Vierling, Rowell, Chen, Dykstra, & Vierling, 2002). Past work has demonstrated that lidar-derived canopy vegetation profiles compare well with ground-based profiles (Harding, Lefsky, Parker, & Blair, 2001). Other studies have shown that canopy vegetation profile metrics are useful for predicting biomass and other structural variables (e.g. Drake, Dubayah, Knox, Clark, & Blair, 2002; Drake et al., 2002; Garcia, Riano, Chuvieco, & Danson, 2010; Hurtt et al., 2004; Jensen et al., 2008; Lefsky et al., 1999; Lefsky et al., 2005, 2006; Means et al., 1999; Nelson, Short, & Valenti, 2004; Tang et al., 2012).

Discrete return lidar instruments are capable of producing several returns per square meter, and using return counts and summed intensities in discrete return lidar voxels (i.e. volumetric pixels) can be aggregated to develop vegetation profiles (Blair & Hofton, 1999). The high density of individual returns has made discrete return lidar data particularly amenable to high spatial resolution digital surface modeling of both ground (e.g. Hodgson, Jensen, Schmidt, Schill, & David, 2003; Hodgson et al., 2005) and forest canopies (e.g. Popescu & Zhao, 2008). Past work has demonstrated that lidar-derived canopy vegetation profiles compare well with ground-based profiles using full waveform lidar (e.g. Harding et al., 2001), and somewhat less-so using discrete return lidar (e.g. Lovell, Jupp, Culvenor, & Coops, 2003; Hopkinson et al., 2013; Sullivan et al., 2014).

Stem biomass comprises the largest fraction of aboveground biomass in mature forests, and it is related to the product of basal area and height. Much work has been done on temperate forest structure using lidar data, such as LAI, habitat quality and other structural parameters that go beyond just biomass estimation (Clawges, Vierling, Vierling, & Rowell, 2008; Jensen et al., 2008; Morsdorf, Kotz, Meier, Itten, & Allgower, 2006). Many of these advances in temperate forests have not been seen in tropical forests because of the lack of lidar collection in tropical regions, difficulty in conducting field based measurements, differences in field based methodology confounding interpretation, lack of ongoing experimental plots for comparison, unique

and unknown historical forest disturbances, and complexity of the structure due to the diversity of tree species (Asner et al., 2013; Chambers et al., 2007; Frolking et al., 2009).

We stress that lidar derived vegetation profiles contain information that provides information on tree stand size distributions in addition to other forest biometric properties (e.g. canopy geometry) (Hunter et al., 2013; Stark et al., 2012). In the tropics, studies have largely focused on height metrics from lidar-derived vegetation profiles, whereas other metrics such as lacunarity and entropy show promise to provide information on disturbance history (Weishampel, Drake, Cooper, Blair, & Hofton, 2007), in addition to biomass (Stark et al., 2012; Zhao, Popescu, & Nelson, 2009). In tropical forests, work using lidar has been conducted at La Selva, Costa Rica to estimate forest structural properties. Discrete return lidar instruments have provided improvements on the estimation of LAI and metrics related to canopy geometry and architecture (Tang et al., 2012; Vierling et al., 2002). Tang et al. (2012) estimated field measured LAI using the entire waveform collected by NASA's Laser Vegetation Imaging Sensor (LVIS) (Dubayah et al., 1997). Dubayah et al. (2010) compared field measured biomass with various lidar estimated height metrics derived from LVIS waveforms. Treuhaft et al. (2010) used Fourier analysis of waveform profiles to estimate biomass. These three studies used LVIS waveform lidar data. Using discrete lidar, Kellner, Clark, and Hubbell (2009) examined gap transition at La Selva, Costa Rica using two datasets 8.5 years apart.

In this study we sought to relate field-measured forest characteristics, including biomass, height, diameter, basal area, and an array of canopy geometric parameters, such as maximum height and crown depth, to measures derived from discrete return lidar data. Previous studies have established relationships between lidar metrics, primarily percentile measures or relative height classes, to field data. We developed a suite of metrics from untransformed and transformed relative vegetation profiles (RVPs) calculated from discrete return airborne lidar data. These metrics are not commonly used and we consider them to be analogous to field-based measurements, such as the number of canopy local maxima in a RVP, measures of canopy vegetation distribution diversity and evenness (entropy), and estimates of gap fraction. We developed a modeling procedure that utilized hypothetical stand characteristics to generate synthetic vegetation profiles that could be compared with profiles developed from field and lidar data. Essentially, this method was used in an effort to estimate stand characteristics by comparing lidar RVPs to a series of modeled RVPs with known stand conditions (e.g. shape and scale of the diameter distribution). We also included lidar coherence metrics pulled from discrete Fourier transforms of untransformed profiles based on the approach of Treuhaft et al. (2010). We expect that these metrics, used in lieu of and in addition to relative height percentiles used in other studies (e.g. Drake et al., 2003; Dubayah et al., 2010), may prove valuable because they account for sub-dominant canopy structure and variability in canopy vegetation profiles.

2. Methods

2.1. Site location

Our study was conducted within the La Selva Biological Station (10° 26′ N, 83° 59′ W), in the Atlantic lowlands of Costa Rica, operated by the Organization for Tropical Studies (McDade & Hartshorn, 1994). Using a set of a priori constraints on site selection and GIS data layers (trails existing studies, water bodies, vegetation type) provided by the La Selva (http://www.ots.ac.cr), twenty plots were randomly selected throughout La Selva on which to measure field-based biometric properties and examine with remotely sensed lidar data (Fig. 1). For ease of access, sites were chosen within 100 m and greater than 30 m of established trails. To address potential issues with local topography, sites were selected that were at least 50 m from rivers and water bodies. To avoid disturbing ongoing long term research, plots were selected so
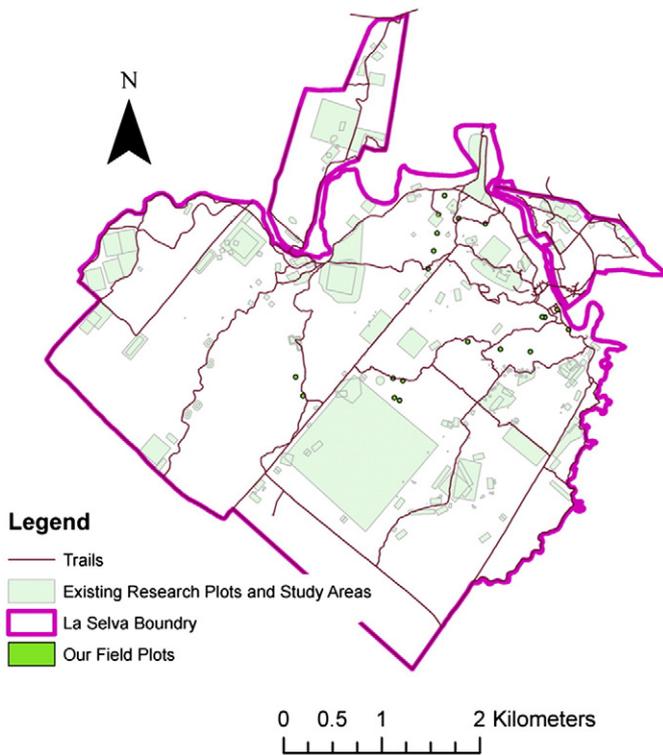
Bitterlich sampling samples trees with probability proportional to basal area, the mean height of the measured trees provides an unbiased estimate of Lorey's height. Average stand properties were calculated following adjustment of individual trees for their sampling frequency (Husch et al., 2003). A summary of plot locations and measurements is presented in Table 2.

Field plot measurements were collected in January 2012. We note that our field data was collected sixteen months after the lidar data collection (September 2009). Our plots were situated in high biomass plots that are likely to not change as much as young secondary forests. In addition, because our plots were variable in plot size, but about 30 m on average, we feel that our estimates using lidar and measurements of field data provide for a reasonable statistical comparison.

Plots were located in old growth, abandoned pasture (approximately 70 years), and logged and secondary forest types. We measured basal area on 20 plots and 80 satellite plots using a variable plot size method. Our stratified sampling design yielded trees of all dbh sizes classes, thus providing a good indication of canopy contribution for comparison with lidar data.

2.3. Lidar and derived parameters

Small-footprint discrete return LIght Detection And Ranging (lidar) data were collected over La Selva Biological Research Station on September 26, 2009 during a three-hour flight for the Tropical Ecology Assessment and Monitoring (TEAM) Network by Northrop Grumman Corporation (Tropical Ecology Assessment & Monitoring (TEAM) Network of Conservation International, 2009). An Optech 3100EA lidar sensor was used to collect data for this study. The sensor was flown at an altitude of 1500 m, yielding a sampling density of approximately 3.5 returns m^{-2} within our study plots. Associated RGB imagery with 0.15 m spatial resolution was acquired during the flight, though RGB data were not used in this study. The aircraft was fitted with an inertial measurement unit, Applanix POSAV 510, to correct for roll, pitch, and yaw, with two GPS base stations and several ground control points for georeferencing. lidar point clouds were classified prior to our accessing the data using Terrasolid 9.0 (Terrasolid, Software for LiDAR processing, 2009). A digital elevation model (DEM) was developed by two-dimensional linear interpolation of all ground-classified lidar returns. Nearest neighbor interpolation was used to estimate the ground elevation of pixels outside of the convex hull of the ground return point cloud. Elevations above ground were calculated for vegetation-classified returns by subtracting the DEM ground elevation for each vegetation return. Following this, we developed RVPs from lidar returns to describe the vertical distribution of plant material within a 30 m radius of plot center on each of 20 plots at La Selva. 1 m binned histograms of lidar returns were normalized then transformed to account for

Fig. 1. Location of plots (green circles) and La Selva Biological Station layout.

that they were at least 25 m away from established study areas. In order to sample for a range of forest types, fourteen old growth forests and six abandoned pasture, logged, and secondary forests (referred to as abandoned pasture, or other forest types from here on) were sampled. Field plots were located using a Garmin 76CSx GPS.

2.2. Field data collection

At each of the twenty plot locations, a cluster of horizontal point samples was deployed using a point double sampling approach, in which counts of trees using Bitterlich samples are used to estimate basal area per hectare at a large number of points but actual tree measurements are taken on a subsample of trees (Oderwald & Jones, 1992). Trees were counted using a Spiegel-relaskop using a basal area factor (BAF) of 4 m^2 ha^{-1} at the plot center and at four satellite plots spaced 30 m from the plot center on each of the cardinal directions (Gregoire, 1998). This sampling method was chosen because the variable plot radius design allows for a stratified sampling of trees that are more likely to contribute to the canopy above a specific point and thus provides better sampling for comparison with remote sensing data. For all trees to be included in our variable plot, we measured diameter at breast height (dbh) using a diameter tape, and total height and height to the base of the live crown using a Vertex hypsometer (Haglof Inc.). For those trees with buttresses that precluded measurement of dbh at the usual height (1.37 m), the diameter was measured outside bark immediately above the buttresses optically using the Spiegel-relaskop at a known distance from the tree (Bitterlich, 1984). These include basal area (area of the cross section of trees at breast height per total area) and quadratic stand diameter (QSD; calculated from plot-level summary data as square root ((ba/n) ∗ (4/pi)) (Husch, Beers, & Kershaw, 2003). Total biomass for each tree was calculated using two sets of allometric equations, those of Brown (1997) and Chave et al. (2005). Estimates of per-hectare values other than basal area were calculated using the basal area ratio approach (Marshall, Iles, & Bell, 2004). Because

Table 1
Description of lidar-derived vertical profile metrics.

Variable	Description
Mean synthetic DBH	Mean dbh of modeled trees in synthetic forest
Synthetic shape	Shape parameter of the best fit Weibull distribution
Coh_1.04	Lidar coherence at a frequency of 1.04 rad/m
Coh_0.88	Lidar coherence at a frequency of 0.88 rad/m
Coh_0.60	Lidar coherence at a frequency of 0.60 rad/m
Coh_0.28	Lidar coherence at a frequency of 0.28 rad/m
Entropy	Forest height diversity within 1 m bins
PAI	Estimated plant area index
Layer count	Number of local maximums in vertical profile
Peak maxima	Elevation of the largest local maximum
Highest maxima	Elevation of the highest local maximum
Layer diff	Elevation difference between highest maxima and lowest maxima
P_{50}	Fiftieth percentile, estimated by interpolation
$P_{50}:L_{max}$	Ratio of P_{50} to the height of the max lidar return

Table 2
Plot locations and field measured characteristics.

Plot	Forest type	Lon	Lat	Basal area	Density	Biomass1	Biomass2	Mean DBH	QSD	Mean height	Lorey's height	Mean crown base height	Mean crown depth	Max height
BP1	OG	−84.005	10.429	28	135	370	464.05	51.2	54.78	24.76	29.8	16.44	8.32	39.1
BP10	OG	−84.006	10.429	28.8	174	362.4	435.77	37.99	41.81	24.06	28.42	16.84	7.22	36.8
BP11	OG	−84.006	10.429	24.8	399	294.9	351.49	24.84	29.89	18.68	28.4	11.58	7.11	36.2
BP2	OG	−84.009	10.426	22.4	471	230.75	243.54	21.61	23.25	21.19	21.62	13.17	8.02	24.4
BP3	OG	−84.025	10.42	21.6	277	255.56	314.6	21.26	27.08	12.24	20.9	9.69	2.55	27.1
BP4	OG	−84.026	10.422	22.4	893	190.3	208.25	13.57	15.1	10.12	15.25	7.6	2.52	24.6
BP5	OG	−84.012	10.426	26.4	300	310.21	365.6	24.47	29.12	13.63	23.36	7.39	6.24	39.3
BP6	OG	−84.007	10.426	18.4	91	233.96	278.79	45.44	47.06	35.93	40.6	24.49	11.44	57.7
BP7	OG	−84.011	10.436	29.6	378	328.98	374.99	22.76	25.95	17.56	22.82	14.29	3.26	36.2
BP8	AP	−84.014	10.436	19.2	119	227.2	254.2	34.47	35.7	22.78	24.63	17.31	5.47	29.7
BP9	OG	−84.004	10.428	28	278	353.2	428.65	35.63	40.56	22.83	31.35	13.64	9.19	45.9
GL1	LOG	−84.015	10.438	20.8	40	285.55	374.26	67.85	71.01	39.2	41.1	23.45	15.75	48.8
GL2	AP	−84.015	10.436	28.8	592	316.37	360.29	21.18	24.54	19.55	26.94	12.65	6.89	46.7
GL3	SEC	−84.016	10.432	26.4	232	326.1	385.58	35.85	39.13	26.6	29.81	20.78	5.82	36.1
GL4	AP	−84.015	10.435	23.2	467	256.77	278.74	25.54	27.61	23.73	29.6	17.7	6.03	34.1
GL5	AP	−84.015	10.433	26.4	709	277.02	291.65	24.44	25.42	21.68	23.38	16.07	5.61	31.2
GL6	OG	−84.018	10.423	18.4	249	210.88	256.49	19.72	24.77	13.86	29.53	8.23	5.62	40.1
GL7	OG	−84.017	10.422	26.4	165	333.94	394.5	45.22	46.44	33.22	34.84	23.64	9.58	45.4
GL8	OG	−84.018	10.421	23.2	459	261.08	320.6	15.74	21.06	18.68	24.25	10.98	7.69	32.7
GL9	OG	−84.017	10.421	27.2	432	319.1	379.57	24	28.72	17.01	24	11.78	5.24	38.3

OG = Old growth, AP = Abandoned plantation, LOG = Logged forest, SEC = Secondary forest.
Biomass1: from Brown (1997), Biomass2: from Chave et al. (2005).

occlusion of plant material, as in MacArthur and Horn (1969). This transformation was recently shown to be functionally similar to survival analysis (Maynard et al., 2013) and was previously shown by Lefsky et al. (1999), using waveform lidar, and using discrete return lidar (_e.g._ Coops et al., 2007; Hilker et al., 2010; Stark et al., 2012), to be equivalent to:

$$PAI(h) = -\ln(1-cover(h)) \tag{1}$$

where cover (h) is the fraction of ground (or in the case of a ground-based sensor, the fraction of sky) that is obscured by vegetation below height, h, and PAI (h) is the plant area index above h. By varying h in 1 m increments, we calculated an estimated cumulative distribution of vegetation occurrence within the canopy. The first derivative of the cumulative distribution provided a relative vegetation profile (_e.g._ Lefsky et al., 1999, Hilker et al., 2010). The MacArthur–Horn vertical line intercept correction was thought to provide an estimate of leaf area index (LAI) where leaf observations could be discriminated from non-photosynthetic vegetation; however, previous studies have shown that the method is not accurate in northern hardwood forests (Aber, 1979b). In the case of lidar, observations of leaf material and other plant organs are not discriminated, so any estimate, however inaccurate, would be an estimate of PAI, as opposed to LAI. In addition to the derivation of the RVP, we calculated an estimate of PAI for the entire canopy.

From transformed and untransformed RVPs, we derived a series of parameters, including some not traditionally used in the statistical comparison of lidar data with field-based vegetation structural components (Table 1). In addition, from the transformed RVPs, we calculated the parameter called layer count using an automated local maximum count, under the assumption that each local maximum in an RVP represents trees from a single height class (_e.g._ Hofton, Minster, & Blair, 2000). A slightly different method using a threshold for gap and canopy has been used to estimate canopy layers (Pekin, Jung, Villanueva-Rivera, Pijanowski, & Ahumada, 2012). Based on the layer count, we calculated the peak maxima as the relative height of the largest maximum, and the highest maxima as the relative height of the highest maximum in each profile. In addition, using interpolation, we estimated the median height of the transformed vertical profile (P_{50}) and calculated a ratio of the height of the maximum lidar return to the median height on each plot ($P_{50}:L_{max}$).

Lastly, we calculated entropy of each RVP. Entropy is a measure commonly used in community ecology research (otherwise known as Shannon's entropy, or Shannon's Diversity Index) and in image processing (_e.g._ Ouma, Tetuko, & Tateishi, 2008; Shannon 1948), but has only seldom been applied in the context of vertical complexity (_e.g._ Stark et al., 2012; Treuhaft et al., 2009). We calculated entropy of RVPs using a sampling frequency (vertical bin size) of 1 m:

$$Entropy = \sum_i -p_i \ln p_i \tag{2}$$

where p_i is the proportion of plant area in height bin _i_. Prior to calculating metrics, a discrete approximation of a Gaussian distribution filter of five bins was applied to transformed profiles to reduce noise.

We calculated Fourier transforms for 1500 discrete frequencies between 0 rad m^{-2} and π rad m^{-2}. Lidar coherence from Fourier transforms at frequencies of 1.04 rad m^{-2} (Coh_1.04) and 0.31 rad m^{-2} (Coh_0.31) was extracted following the results of Treuhaft et al. (2010, 2013). These frequencies correspond to vertical wavelengths of 6 m and 20 m, respectively. Theoretically, Fourier transform amplitudes at given frequencies correspond to variability in vertical forest structure at associated spatial wavelengths. We elected to use these frequencies because normalized Fourier transform amplitudes at cycle frequencies corresponding approximately to strong forest height signals (_i.e._ mean tree height and crown depth) have been shown to be correlated with biomass (Treuhaft et al., 2010). Analysis of Fourier transforms was performed to identify additional frequencies of interest based on amplitude range and coefficient of variation across plots (see Fig. 4 in Results).

2.4. Synthetic forest algorithm

Tree height and the canopy foliage distribution are highly correlated to trunk diameter (Asner et al., 2002; Broadbent et al., 2008; Feldpausch et al., 2010). The comparison of successive trunk diameter classes of trees is often used as an indicator of forest dynamics, though caution must be exercised in making simple assumptions about age–diameter relationships (Oliver & Larson, 1996). Diameter distribution in successive size classes has often been associated with forest light dynamics (Montgomery & Chazdon, 2001; Stark et al., 2012; Terborgh, 1985). Old-growth forests that are assumed to be at or near a steady state are often modeled using a "q ratio" approach, in which the ratio between the number of trees in successive diameter classes is roughly constant (Meyer & Stevenson, 1943). The first formal expression of the q ratio

was made by the French forester de Liocourt (1898), who used the term to describe the "quotient of diminution" or rate of change between numbers of trees in successive diameter classes, i.e., $q = N_j / N_{j+1}$, where N_j is the number of trees in the jth diameter class. Later authors emphasized the prevalence of a constant q, which gives rise to an exponential diameter distribution (Keller, Palace, & Hurtt, 2001; Meyer, 1943; Meyer, 1952; Meyer & Stevenson, 1943).

Although much of the literature on mixed-age stands emphasizes the constant q formulation, de Liocourt (1898) himself found that q varied within stands, and much recent attention has focused on alternative diameter distributions. These include the Weibull (Bailey & Dell, 1973), which includes the constant-q as a special case, and the Burr, which can represent "rotated sigmoid" distributions that appear to be common in many uneven-aged forests (Gove, Ducey, Leak, & Zhang, 2008). These distributions all have closed-form expressions, and can be estimated by maximum likelihood and used in stand simulations. It may also be possible to estimate the number and size distribution of small trees that are not easily resolved (sub-canopy) from the size distribution of those that are (McGarrigle, Kershaw, Lavigne, Weiskittel, & Ducey, 2011).

In an effort to cull more information from the vegetation profile derived from the discrete lidar data (Section 2.3) a modified version of a previously developed synthetic forest algorithm was used (Morton et al., 2014a). Using multiple geometric series we generated vegetation profiles using a three-dimensional canopy model. Our canopy model uses trunk size (dbh) and allometric equations of associated crown depth, width and height to generate a three dimensional canopy. We generate an ellipsoid in three dimensional space based on these parameters (dbh and crown geometry) to develop a forest canopy (Fig. 2). Allometric equations from Asner et al. (2002) were used for estimating crown dimensions from dbh. Using this synthetic forest algorithm we were interested in examining the hypothetical forest stand dbh distribution. Because plots often represent the variability of disturbances and regrowth in a forest, we decided that using the model to examine the hypothetical forest stand distribution was an interesting approach to delving into understanding the discrete derived vegetation profile. To accomplish this, synthetic forests (1 km²) were developed with a tree count of approximately 200,000 trees, based on Weibull distributions. The Weibull distribution has two parameters, where the shape parameter is designated (ß), and the mean of the distribution termed (α) (Bailey & Dell, 1973). Our shape parameter (ß), ranged from 0.8 to 1.2 (bin size 1 cm) in increments of 0.1 m, and mean of the distribution varied from the 8 cm dbh to 150 cm. Individual trees pulled randomly from the distribution ranged from 0 cm to 500 cm dbh (e.g. Fig. 3). Spacing of trees was controlled using a decision scheme to restrict crown overlap to less than half of the horizontal radius of any crown (Hanus, Hann, & Marshall, 1998; Morton et al., 2014b). This resulted in canopy gap values on par with literature (Morton et al., 2014b). Vertical profiles from synthetic forests were derived by aggregating the horizontal distribution of modeled canopies. Synthetic

vegetation profiles were normalized and compared to transformed lidar RVPs by a least-squares goodness-of-fit metric to identify the best-fit synthetic profile for each lidar RVP. The shape parameter and the mean DBH of the input trees to the best-fit synthetic profile were retrieved and included as input parameters for our analysis. Though these parameters were representative of hypothetical forests, they are parameters that could be used to develop additional properties of the lidar derived vegetation profile. Our effort here was to extract additional metrics from the lidar waveform for parameters is estimating field-based measured forest structural properties.

2.5. Statistical analysis

We developed multiple regression models using forward stepwise regression with Bayesian information criteria (BIC) for variable inclusion in the model (Claeskens & Hjort, 2008). We used field measured biometric properties collected using a variable plot radius approach described in Section 2.2 for comparison with the transformed RVP from the lidar data. In addition we compared lidar transformed RVPs to profiles derived from the synthetic forest algorithm to develop additional metrics for examining relationships. We note that there are numerous other variables that are available for the development of multiple regression models, but we chose these variables to explore the use of our synthetic forest output and unique parameters not normally used in lidar comparison with forest biometric properties. Data were extracted using LAS tools (www.cs.unc.edu/~isenburg/lastools/). All derived lidar metrics were calculated in Python 2.7. Statistical analyses were performed in Python (Python Software Foundation, Python version 2.7) and JMP 10 (SAS).

3. Results

3.1. Field data

We measured a total of 137 trees for dbh, crown height, crown depth, crown width, and location for all twenty plots. Basal area ranged from a minimum of 18.4 m² ha⁻¹ on an old growth plot to a maximum of 29.6 m² ha⁻¹ also on an old growth plot, with a mean basal area across all plots of 24.5 m² ha⁻¹ and a standard deviation of 3.6 m² ha⁻¹. Old growth plots averaged 24.6 m² ha⁻¹ and other forest types averaged 24.13 m² ha⁻¹. Tree density ranged from 40 to 893 trees ha⁻¹, with a mean of 343 trees ha⁻¹ and standard deviation of 217 trees ha⁻¹. The minimum density occurred on a logged plot, and the maximum density was in an old growth plot. The large range in tree density may be an artifact of a large range in mean DBH, which ranged from a minimum of 13.6 cm to a maximum of 67.9 cm, with a mean of 30.6 cm across all plots, and means of 28.8 cm and 34.8 cm within old growth and all other plot types, respectively. Mean tree height ranged from 10.1 m to 39.2 m, with a mean and standard deviation of 21.87 m and 7.6 m across all plots, and means of 20.27 m and 25.6 m within old growth and other types, respectively. Mean crown depth ranged from 2.5 m to 15.8 m, with a mean crown depth of 7 m and standard deviation of 3.1 m. Mean crown depth within old growth plots was 6.7 m, and within other plot types mean crown depth was 7.6 m. Maximum height ranged from 24.4 m to 57.7 m, with the minimum and maximum occurring on old growth plots. Mean maximum height across all plots was 37.5 m with a standard deviation of 8.4 m. Within different plot types, mean maximum height was nearly unchanged, with a mean maximum of 37.4 m and 37.8 m within old growth and other plot types, respectively. Estimated above ground biomass using the equation from Brown (1997) (Biomass1) ranged from 190 to 370 Mg ha⁻¹ with a mean of 287.2 Mg ha⁻¹ and standard deviation of 52.47 Mg ha⁻¹. Within forest type means were 289.7 Mg ha⁻¹ and 281.5 Mg ha⁻¹ for old growth and other plot types, respectively. Estimated above ground biomass using a second equation (Biomass2, from Chave et al., 2005) ranged from 208.25 to 464 Mg ha⁻¹, with a

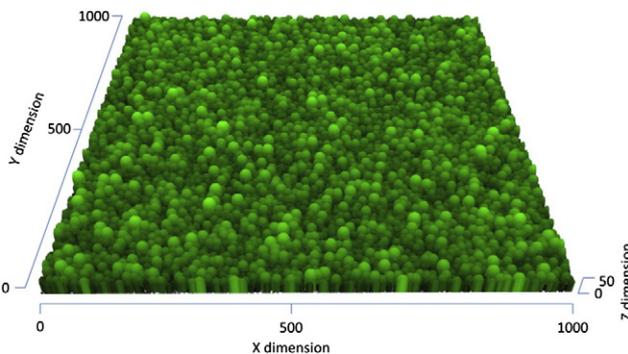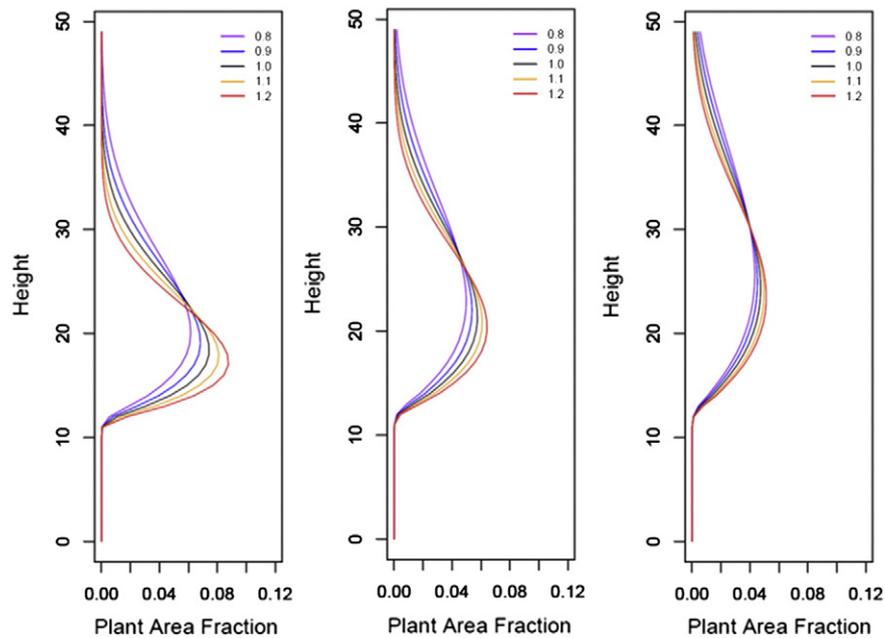**Fig. 2.** A synthetic forest example.

Fig. 3. Synthetic canopy profiles generated using allometric relationships between crown width and both tree height and height to the bottom of the canopy. Shown here are profiles with mean diameters of 15 cm (left), 30 cm (middle) and 55 cm (right), with the shape parameter of the Weibull distribution varied from 0.8 to 1.2 in increments of 0.1.

mean of 338 Mg ha^{-1} and a standard deviation of 70.5 Mg ha^{-1}. We note that the Chave equation (Biomass2) uses height in addition to dbh to estimate biomass. Within forest type means were 344.1 and 324.1 Mg ha^{-1} for old growth and other types, respectively. For both biomass estimates, the maximum and minimum estimated biomass occurred in old growth plots.

3.2. Lidar data analysis

Summaries of the derived lidar metrics and the results from the synthetic profile comparison are found in Table 3. Estimated mean dbh from synthetic profiles ranged from 9.41 cm to 59.99 cm, with a mean of 14.4 cm and a standard deviation of 5.3 cm. Means within different forest types were not considerably different (14.4 cm^2 in old growth and 14.2 cm^2 in other plot types). Entropy of RVPs ranged from 2.78

to 3.44, with a mean of 3.1 and a standard deviation of 0.19. Entropy within old growth plots averaged 3.15 and 3.0 within other plot types; however both the maximum and minimum entropy occurred on old growth plots. Estimated PAI ranged from 3.2 to 4.36, with a mean PAI of 3.75 and standard deviation of 0.3 across all plots. Means within plot types were not considerably different (3.72 within old growth plots and 3.81 within other plot types). Layer count ranged from 1 to 4 layers, with a mean count of 2.6 and standard deviation of 0.75. The mean number of layers in old growth plots was higher than in other plot types (2.7 and 2.3), however both the minimum and maximum number of layers occurred in old growth plots. The peak measured maximum ranged from 10 m to 31 m (both on old growth plots), with a mean of 16 m and a standard deviation of 6.05 m. The mean peak occurred at 15.1 m on old growth plots and at 18 m on other plot types. The mean height of P$_{50}$ occurred at 18.1 m, with a standard deviation

Table 3
Vertical profile derived lidar metrics.

Plot	Mean synthetic DBH	Synthetic shape	Coh_1.04	Coh_0.88	Coh_0.60	Coh_0.28	Entropy	PAI	Layer count	Peak maxima	Highest maxima	Layer diff	P$_{50}$	L$_{max}$:P$_{50}$
BP1	14.76	0.8	0.071	0.025	0.094	0.134	3.26	3.94	4	21	27	17	22.51	0.57
BP10	11.35	0.8	0.058	0.081	0.094	0.238	3.14	3.68	3	13	26	16	16.87	0.43
BP11	11.37	0.8	0.048	0.077	0.099	0.206	3.23	4	3	10	19	9	19.56	0.47
BP2	9.41	1.2	0.064	0.060	0.149	0.508	2.99	3.76	3	14	41	27	17.35	0.39
BP3	9.66	1.1	0.117	0.125	0.163	0.376	2.9	3.6	3	10	29	19	14.11	0.44
BP4	9.41	1.2	0.080	0.105	0.169	0.440	2.78	3.22	1	10	10	0	15.54	0.50
BP5	10.49	0.9	0.098	0.097	0.150	0.243	3.05	3.78	2	11	16	5	18.48	0.48
BP6	59.99	1.1	0.022	0.012	0.109	0.102	3.44	3.92	4	31	45	33	23.51	0.49
BP7	21.3	0.8	0.052	0.050	0.125	0.093	3.43	4.36	3	23	43	33	25.03	0.51
BP8	10.49	0.9	0.043	0.069	0.056	0.274	3.14	3.88	3	18	41	27	19.52	0.43
BP9	14.76	0.8	0.060	0.063	0.105	0.124	3.24	3.2	2	22	22	12	21.45	0.52
GL1	18.21	0.8	0.074	0.047	0.074	0.079	3.25	4.08	3	22	22	12	24.74	0.63
GL2	9.66	1.1	0.039	0.056	0.096	0.462	2.82	3.62	2	17	19	2	18.66	0.60
GL3	26.35	1.2	0.010	0.016	0.177	0.367	2.99	3.7	2	22	22	8	23.27	0.66
GL4	10.43	0.9	0.058	0.100	0.027	0.334	2.95	3.87	2	18	18	8	19.44	0.61
GL5	10.9	1	0.085	0.097	0.225	0.331	2.86	3.85	2	11	20	9	18.11	0.58
GL6	19.17	0.8	0.074	0.060	0.109	0.129	3.17	3.27	2	10	29	19	19.54	0.55
GL7	11.35	0.8	0.085	0.081	0.115	0.241	3.13	3.38	2	10	25	15	18.06	0.46
GL8	11.35	0.8	0.072	0.124	0.159	0.315	3.2	3.98	3	10	31	21	16.20	0.39
GL9	10.04	1	0.076	0.094	0.066	0.389	3.13	3.92	3	17	41	31	18.53	0.42

Note: coherence (Coh) metrics derived from untransformed vertical profiles, other metrics derived from MacArthur–Horn transformed profiles.

of 18.1 m and a range of 14.9 m to 24.9 m, both occurred on old growth plots. The within type mean P_{50} was 18 m on old growth plots, and 18.3 m on other plot types.

3.3. Fourier transforms

At a frequency of 0.31 rad m^{-1} coherence (vertical wavelength of 20 m) ranged from 0.024 to 0.413 with the minimum in old growth and maximum on an abandoned plantation plot. Mean coherence at this frequency was 0.23 with standard deviation of 0.1. At a frequency of 1.04 rad m^{-1} coherence ranged from 0.01 to 0.117 with mean of 0.024 and a standard deviation of 0.011. Old growth plots had an average of 0.051 and other plot types had an average of 0.070. In addition to transform frequencies sampled based on results from previous studies (Treuhaft et al., 2010), we identified three frequencies to include in regression analyses. We found large peaks in range and coefficient of variation at approximately 0.28 rad m^{-2}, 0.60 rad m^{-2}, and 0.88 m^{-2}, corresponding to vertical wavelengths of 23 m, 10.5 m and 7.25 m, respectively (Fig. 4). At 0.276 rad m^{-2}, the magnitude of the Fourier transform ranged from 0.079 to 0.508 with a mean of 0.269 and standard deviation of 0.132. At 0.599 rad m^{-2}, Fourier transform magnitude ranged from 0.027 to 0.225 with a mean of 0.118 and standard deviation of 0.047. Lastly, at 0.879 rad m^{-2}, we found a mean Fourier transform magnitude of 0.072 with a standard deviation of 0.032, ranging from 0.012 to 0.125. The vertical wavelengths corresponding to these frequencies approximated mean tree height (21.87 m), mean crown depth (7 m), and the height of profile truncation (10 m).

3.4. Regression analysis

We observed moderate to strong relationships between some field-measured traits and a suite of metrics derived from the vegetation profiles we developed using lidar data (lidar metrics) (Tables 4 and 5). Notably, however, the candidate metrics did not converge on a statistically significant model to estimate basal area across all plots. We found a significant relationships between metrics and one of the biomass estimates using only the synthetic shape parameter for each (biomass1: $r^2 = 0.17$,

$p = 0.069$, $RMSE = 49.05$ Mg ha^{-1}; biomass2: $r^2 = 0.23$, $p = 0.031$, $RMSE = 63.43$ Mg ha^{-1}). In addition, we found a strong relationship between lidar entropy and tree density ($r^2 = 0.43$, $p = 0.002$, $RMSE = 167.88$ n ha^{-1}) and between lidar metrics and both mean dbh and quadratic stand diameter (QSD; square root ((ba/n) * (4/pi))) ($r^2 = 0.51$, $p = 0.004$, $RMSE = 9.47$ cm; $r^2 = 0.43$, $p = 0.003$, $RMSE = 10.04$ m^2, respectively). Lorey's height and maximum height were both significantly related to several lidar metrics. Lorey's height and maximum height shared five variables in the final model, while Lorey's height estimates included two additional variables that were not used for estimating maximum height (Lorey's height: $r^2 = 0.67$, $p = 0.003$, $RMSE = 3.65$ m; max height: $r^2 = 0.68$, $p = 0.001$, $RMSE = 4.79$ m). Significant relationships were also found between the mean crown base height and the lidar peak maxima ($r^2 = 0.37$, $p = 0.005$, $RMSE = 4.29$ m), maximum crown base height and both synthetic forest variables ($r^2 = 0.55$, $p < 0.001$, $RMSE = 3.61$ m), minimum crown base height and P_{50} ($r^2 = 0.32$, $p = 0.01$, $RMSE = 3.65$ m), minimum tree height ($r^2 = 0.33$, $p = 0.008$, $RMSE = 5.32$ m), and minimum crown depth and ($r^2 = 0.38$, $p = 0.004$, $RMSE = 2.18$ m). However, no significant relationship was found for maximum crown depth ($r^2 = 0.17$, $p = 0.07$, $RMSE = 4.5$ m).

4. Discussion

Our field-based measurements are comparable with those found from other studies at La Selva (Clark, Roberts, Ewel, & Clark, 2011). Mean biomass measured in our study (ranging 190 to 370 Mg ha^{-1} with a mean of 287.2 Mg ha^{-1} and standard deviation of 52.47 Mg ha^{-1}) was high compared to Clark and Clark (2000) (between 160 and 182 Mg ha^{-1}), but similar to that in Treuhaft et al. (2010) (229 Mg ha^{-1}). Dubayah et al. (2010) measured biomass values ranging from 90.73–194.95 Mg ha^{-1} to 118.88–197.81 Mg ha^{-1}. Our focus of plot selection was on older growth forests and plots that were not disturbed by recent blowdowns or gap-phase disturbances. This was done to allow for comparison with lidar collected data two years prior to our field measurements, and this should cause our estimates to be higher than surveys that include disturbances such individual tree falls and blowdowns (Espírito-Santo et al., 2014). Logged and abandoned plantation and pasture plots in our study (BP8, GL2–5) had high biomass for such disturbed secondary forests. This was because the disturbances were minor, were many years old, and with selective logging only having removed about 1 individual per hectare (Palace, Keller, Asner, Silva, & Passos, 2007). Pastures and plantations often leave larger trees for shade for cattle or specific crops in the tropics and these plots had large trees, which contributed a high proportion to the biomass estimates for these plots. These plots were disturbed approximately 70 years ago (McDade, Bawa, Hespenheide, & Hartshorn, 1994) and have had ample time for individuals from secondary growth to fill in canopy space and grow in girth. However, if we were to have tracked individual species, where pioneer species often have a lower biomass due to less dense wood, our biomass estimates might have been reduced. Basal area estimates in our study were similar to those from other studies (24.5 m^2 ha^{-1} in this study, and 26 m^2 ha^{-1} in Clark & Clark, 2000). Canopy height was consistent with that found in Hurtt et al. (2004), which was approximately 29 m. Many of the field measured canopy geometric properties have not been collected at La Selva, but were comparable to results from tropical forests in Amazonia and the pan-tropical regions (Asner et al., 2002; Broadbent et al., 2008; Feldpausch et al., 2010; Palace, Keller, & Silva, 2008).

We developed multiple linear regressions to explore relationships and predict field-measured forest biometric properties from discrete return airborne lidar data. The biometric properties we examined included more than just forest height and stand biomass. These expanded biometric properties encompassed average dbh, basal area, and canopy height and geometry metrics. The regression models were built using both common and new parameters we extracted from the lidar data.
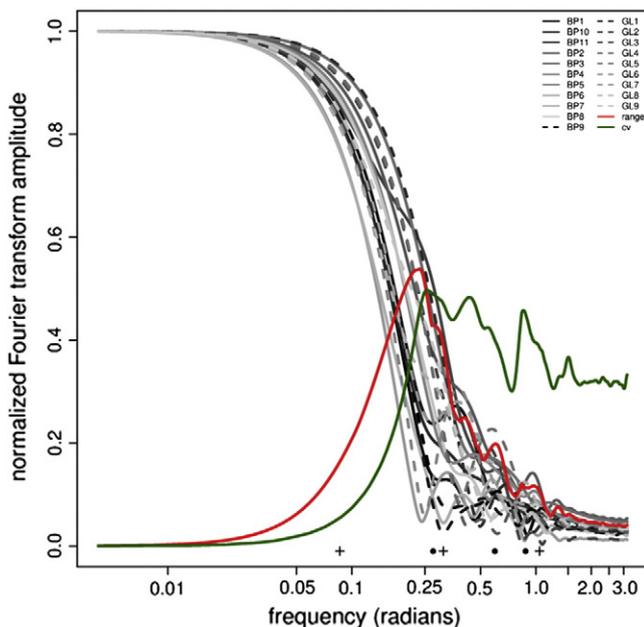
Fig. 4. Fourier transforms of twenty vegetation profiles (grayscale), with range (max–min coherence, red) and coefficient of variation (green) of plots for all frequencies overlaid. Sampled frequencies are marked along the x-axis with crosses (from Treuhaft et al., 2010) and circles (identified in this study).

Table 4
Forward stepwise regression estimates.

	Intercept	Mean synthetic DBH	Synthetic shape	Coh_1.04	Coh_0.88	Coh_0.60	Coh_0.28	Entropy	PAI	Layer count	Peak maxima	Highest maxima	Layer diff	P$_{50}$
Biomass1	**417.63**	–	−138.74	–	–	–	–	**–**	–	–	–	–	–	–
Biomass2	**541.90**	–	−216.83	–	–	–	–	**–**	–	–	–	–	–	–
Tree density	**2751.60**	–	–	–	–	–	–	–	**−775.74**	–	–	–	–	–
Mean DBH	20.49	–	–	–	–	–	–	–	−17.34	**13.94**	–	−0.61	–	**2.85**
QSD	**58.15**	–	–	–	−155.39	–	−46.59	–	**–**	**–**	–	–	–	**–**
Mean height	**10.02**	–	–	–	–	–	–	–	–	–	0.74	–	–	–
Lorey's height	**55.67**	**0.65**	−42.19	121.67	**−123.55**	−42.61	42.31	–	**–**	–	–	–	−0.24	–
Mean crown base height	**6.45**	–	–	–	–	–	–	–	–	–	**0.53**	–	–	–
Mean crown depth	−2.42	**–**	–	–	–	–	–	–	–	–	–	–	–	0.48
Max height	**34.48**	**0.78**	−30.75	142.76	–	−55.82	–	–	**–**	–	–	2.00	−2.32	–
Max crown Base height	**34.91**	**0.34**	−15.31	–	–	–	–	–	–	–	–	–	–	–
Max crown depth	**18.27**	–	–	–	−61.01	–	–	–	–	–	–	–	–	–
Min height	**25.31**	–	–	–	**−111.55**	–	–	–	–	**–**	–	–	–	–
Min crown base height	−4.48	–	–	–	–	–	–	–	–	**–**	–	–	–	**0.80**
Min crown depth	**−23.35**	–	–	–	–	–	–	**8.95**	–	–	–	–	–	–

p > 0.05, **p < 0.05**, **p < 0.01**.

These include number and location of canopy layers, profile entropy, and a synthetic vegetation profile. The synthetic vegetation profile successfully allowed for theoretical stand distributions to be compared with vegetation profiles developed from discrete lidar data. This was specifically used to tease out additional information from the lidar profile. In essence, the synthetic forest algorithm develops numerous vegetation profiles based on two parameters from a hypothetical model. The two parameters (shape and mean of a forest dbh distribution) in this model are indicative of the thickness of the vegetation profile and the overall height location. This is because dbh and height of vegetation are related; however measures related to the diameter distribution integrate complex details of forest structure properties that are more informative than maximum height. The distribution of trees in various dbh classes represented by the Weibull distribution used in our synthetic forest model represent the canopy structure and vegetation profile of hypothetical forests. Using least-squares we select the vegetation profile with the best fit to that of the lidar profile. The two variables in the synthetic forest model provided information that was used in estimating biomasss, canopy depth, and base of the canopy height as discussed below.

We found that almost all of the field-based forest biometric properties we measured were able to be estimated using parameters derived from discrete return lidar data using multiple regression models. The exception was basal area. Some models utilized up to seven parameters (Lorey's height) and some used only one parameter (biomass, tree density, and all of the minimum canopy geometric indices). We found that many parameters that are unique to our study were selected for inclusion in these models. These include canopy layer properties, synthetic forest profile information, and Fourier analysis parameters. We note

Table 5
Forward stepwise regression results.

Variable	p-value	r^2	RMSE	BIC
Biomass1	0.069	0.17	49.05	219.4
Biomass2	0.031	0.23	63.43	229.6
Tree density	0.002	0.43	167.88	268.6
Mean DBH	0.004	0.51	9.47	158.9
QSD	0.003	0.43	10.04	157.8
Mean height	0.006	0.35	6.31	137.4
Lorey's height	0.003	0.67	3.65	126.6
Mean crown base height	0.005	0.37	4.29	121.9
Mean crown depth	0.033	0.23	2.75	104.2
Max height	0.001	0.68	4.79	134.8
Max crown base height	0.000	0.55	3.61	116.8
Max crown depth	0.071	0.17	4.50	123.8
Min height	0.008	0.33	5.32	130.5
Min crown base height	0.010	0.32	3.65	115.4
Min crown depth	0.004	0.38	2.18	94.8

that biomass estimation did not utilize any height parameters derived from the lidar data, but used the vegetation profile shape generated from our synthetic forest procedure. Our synthetic dbh parameter was only insignificantly, albeit positively, associated with field measured dbh and the synthetic shape parameter was significant and negatively associated with biomass. The shape parameter provides information on the tree trunk size ratios between binned classes and thus is an indication of the proportion of large to small trees. Thus, a higher percentage of larger trees (or lower shape value) is related to a higher biomass. The location of vegetation in a height profile is also related to the shape of the profile, because it changes with the larger ratio of larger trees in the dbh size distribution.

The development of a synthetic forest profile based on Weibull distributions of dbh and allometric equations to describe canopy geometry provided a unique and novel means to compare lidar-based vegetation profiles and a composite of forest structure. This process has the potential to effectively extract a dbh distribution and mean dbh estimate from vertical distributions of plant material. Considering the consistency with which it has been related to forest characteristics such as height and biomass, estimating mean dbh and dbh distributions is particularly valuable. In this study, however, mean synthetic dbh was poorly correlated with mean field dbh ($r^2 = 0.13$, $p = 0.11$). This is likely due to the poor allometric equations for trees at smaller size classes and the resulting uncertainties inherent in understory biomass contribution. Still, canopy height has been shown to be correlated with tree diameter in tropical forests (e.g. Chave et al., 2005), and in this study we found mean synthetic dbh to scale positively with three forest height characteristics. Because height and dbh are positively associated, we expect that increases in the shape parameter result in shorter synthetic forests, and this is supported by our regression analysis. A weakness to our approach of using measured vertical vegetation distribution is that it is still only a relative measure. While there have been some efforts to better the accuracy of estimates of vegetation parameters such as PAI or LAI (e.g. Maynard et al., 2013) further improvement could prove useful for remote biomass estimation.

It is worth noting that our algorithm does not account for disturbances which alter diameter distributions and demographics. In addition, local gap phase dynamics on smaller plots may not be easily compared with results from theoretical stand distributions used in our synthetic forest. For this reason understanding the changes over the landscape that larger plot size plays in a lidar vegetation profile and the variability in field plots is important. By addressing stochastic processes at varying scales pertinent to the forest of interest in future iterations of the algorithm, we hope to improve our results. For example, accounting for tree to tree variability in crown shape and vegetation distribution caused by branch sloughing would be expected to influence tree crown profiles and aggregated synthetic forest profiles (Palace,

Keller, & Silva, 2008). Addressing larger scale disturbances, such as blow down events, would be expected to influence aggregated profiles. These events would influence synthetic forest demographics and may be of particular interest in the context of addressing plot to plot variability within these datasets. To this end, repeat flights of high resolution lidar sensors may be particularly helpful for characterizing forest change (e.g. Kellner et al., 2009; Hall et al., 2011, Sullivan et al., 2014). We note that there have been additional airborne lidar data collected at La Selva collected in 1998 and 2005. These include another discrete lidar dataset (Kellner et al., 2009) and also full waveform lidar from LVIS (Blair & Hofton, 1999; Dubayah et al., 2010). A multivariate analysis of similarities between these different lidar data platforms and changes over time is presented in Sullivan et al. (2014).

Generation of synthetic forests and parameters pulled directly from lidar vertical profiles proved useful in this study. In particular, our estimates of canopy maximums, PAI, entropy, and the Fourier transform analysis provide evidence that parameters typically not used in these types of analyses are of great potential value. Entropy was the only significant variable for estimating tree density and minimum crown depth. Trees exhibit space competition for physical canopy space (Oliver & Larson, 1996) and there may be an underlying optimal packing of canopy foliage in a given space (Niinemets & Anten, 2009). This supports the concept that there is canopy space packing in the forest and this may relate to the density of trees.

Our work offers some support to the notion that canopy signal detection in vertical waveforms – via coherence of Fourier transforms – is informative of forest structure across horizontal space. Relating metrics from Fourier transforms to plot characteristics is a fairly new concept. Previous work has shown that particular frequencies, approximately similar to those used in this study, have exhibited strong relationships with biomass (Treuhaft et al., 2010, 2013, 2015). Higher spatial frequencies are associated with lower vertical wavelengths, and the magnitudes of the Fourier transform (i.e. coherence) are indicative of the strength of the profile at that frequency. Our results support the utility of Fourier transforms of RVPs. Using Fourier transforms, we identified heights approximately corresponding to mean tree height (21.87 m) and canopy depth (7 m) based on variability between plots. Coherence at these phases was particularly useful for estimating tree heights and crown depth.

We were unable to develop a statistically significant relationship between lidar metrics and basal area. Basal area depends on the number of trees and on the diameter distribution; an infinite number of diameter distributions can share the same second moment about the origin and hence the same basal area for a given number of trees per ha. Thus, even ignoring canopy plasticity of individual trees, there can be a wide range of vertical canopy structures associated with the same basal area. Within the context of our synthetic canopy model, there are multiple parameter configurations that can lead to the same basal area value, making it a difficult forest structural parameter to estimate. Moreover, allometric relationships between crown morphology and dbh are not fixed, but dynamic, and strongly mediated by crown length (Mäkelä & Valentine, 2006). Natural gap formation and anthropogenic disturbances (such as logging) often create small to large canopy gaps, allowing changes in crown morphology of adjacent trees and significantly altering relations between canopy structure and dbh size distributions over moderate spatial scales that can take long times to equilibrate. Considering the influence of disturbances on vertical canopy vegetation distribution in La Selva and other tropical forests (e.g. Kellner et al., 2009), precise and accurate remote estimation of diameter distributions at small spatial scales (and therefore basal area) can quickly become complicated. With this in mind, using a rapid modeling procedure such as our synthetic forests, may prove useful for estimating expected distributions and could provide a radiation point for further efforts to model true diameter distribution.

The application of lidar remote sensing to map aboveground biomass in forest ecosystems has expanded considerably over the last decade. Past works have suggested a lack of saturation of the lidar signal with biomass, and documented its application over a broad range of forest biomes (e.g. Boudreau et al., 2008; Drake, Dubayah, Clark, et al., 2002; Gonzalez et al., 2010; Lefsky et al., 2005). Crown-weighted height measurements such as Lorey's height have been proposed as the best proxies for biomass (Saatchi et al., 2011). These relationships are, however, derived empirically with plot data and in the absence of a-priori expectations rooted on ecological principles. In particular, it is not clear whether the documented relationships are driven by resource gradients, elevation gradients, or forest disturbance.

It is well known that information pulled from full waveform lidar footprints and discrete return lidar data are related to field measured height (e.g. Drake, Dubayah, Clark, et al., 2002; Drake, Dubayah, Knox, Clark, & Blair, 2002; Drake et al., 2003; Lefsky et al., 1999). Because of broader crowns, problems associated with missing the highest vegetation within stands are less frequently manifested in tropical forests compared to conifer forests where studies have previously been conducted (Gonzalez et al., 2010; Lefsky et al., 1999). As a result, we found that two of our strongest relationships resulted from regression of lidar metrics against Lorey's height and plot maximum height. However, contrary to previous studies, we could not estimate one of our estimates of field biomass using height metrics derived directly from lidar profiles. Although pan-tropical studies have shown that height and biomass associate positively at the plot scale (Lefsky et al., 2006, Saatchi et al., 2011), within study sites this may not be the case. In fact, field data in this study support this idea; we found no relationship between field-measured height and depth variables and biomass using a simple linear regression ($r^2 = 0.18$, $p = 0.06$). The poor correlations found here and in other studies (Treuhaft et al., 2010) emphasize the need to reevaluate height metrics from lidar data and seek alternative variables for estimating forest structure, with an eye toward characterizing biomass at more local scales. In this regard, a modified iteration of the modeling approach presented here may be particularly useful. We also note that many studies that relate biomass and height examine sites with widely ranging values of both biomass and height. This can add to a strong regression building exercise, but it does not tease out the minute variation found in many older growth tropical forests, where biomass variation is limited and forest height becomes increasingly decoupled with biomass. We suggest that lidar derived height metrics alone are insufficient for estimating biomass within a tropical forest because of the lack of variation across localized landscapes. Furthermore, our study suggests that there are many parameters that can be gleaned from lidar data that prove more informative of forest biometric properties.

5. Conclusion

In this paper, we presented the results of work that used a fused lidar metric and relative vegetation profile modeling approach to estimate forest structure. We found that using information generated from a full lidar profile provided additional avenues for the prediction of field based forest parameters. Although the results associated with the synthetic forest algorithm show room for improvement, we feel that there is promise for similar approaches in future efforts. Assumptions of crown shape, vegetation distribution, and stochasticity need to be addressed by incorporating disturbance regimes of varying scales from tree to stand level. Because the synthetic forest algorithm we developed is for large regions (1 km^2), we plan to exploit the spatial component of the synthetic forests to address questions regarding the influence of sampling schemes on estimates of forest structure. Lastly, our synthetic forest algorithm has potential for global utility by the ability to change crown geometry allometry for different regions. We stress that the high resolution lidar data possesses an often underutilized component, the relative vegetation profile, which is inherently linked to forest dynamics and ecological processes that are exhibited in the structural properties of a forest.

Acknowledgments

References

Aber, J.D. (1979a). Foliage-height profiles and succession in northern hardwood forests. *Ecology, 60*(1), 18–23.

Aber, J.D. (1979b). A method for estimating foliage-height profiles in broad-leaved forests. *Ecology, 67*(1), 35–40.

Asner, G.P. (2001). Cloud cover in Landsat observations of the Brazilian Amazon. *International Journal of Remote Sensing, 22*(18), 3855–3862.

Asner, G.P. (2011). Painting the world REDD: Addressing scientific barriers to monitoring emissions from tropical forests. *Environmental Research Letters, 9*(2). http://dx.doi.org/10.1088/1748-9326/6/2/021002.

Asner, G.P., Mascaro, J., Anderson, C., Knapp, D.E., Martin, R.E., Kennedy-Bowdoin, T., et al. (2013). High-fidelity national carbon mapping for resource management and REDD+. *Carbon Balance and Management, 8*(7). http://dx.doi.org/10.1186/1750-0680-8-7 (2013).

Asner, G., Palace, M., Keller, M., Pereira, M., Silva, J., & Zweede, J. (2002). Estimating canopy structure in an Amazon forest from laser rangefinder and IKONOS satellite observations. *Biotropica, 34*(4), 483–492.

Bailey, R.L., & Dell, T.R. (1973). Quantifying diameter distributions with the Weibull function. *Forest Science, 19*(2), 97–104.

Berenguer, E., Ferreira, J., Gardner, T.A., Aragão, L.E.O.C., De Camargo, P.B., Cerri, C.E., et al. (2014). A large-scale field assessment of carbon stocks in human-modified tropical forests. *Global Change Biology.* http://dx.doi.org/10.1111/gcb.12627.

Bitterlich, W. (1984). *The relascope idea: Relative measurements in forestry* (1st ed.). Slough, UK: Commonwealth Agricultural Bureaux.

Blair, J.B., & Hofton, M.A. (1999). Modeling laser altimeter return waveforms over complex vegetation using high-resolution elevation data. *Geophysical Research Letters, 26*(16), 2509–2512.

Boudreau, J., Nelson, R.F., Margolis, H.A., Beaudoin, A., Guindon, L., & Kimes, D.S. (2008). Regional aboveground biomass using airborne and spaceborne lidar in Quebec. *Remote Sensing of Environment, 112*(10), 3875–3890.

Broadbent, E.N., Asner, G.P., Peña-Claros, M., Palace, M., & Soriano, M. (2008). Spatial partitioning of biomass and diversity in a lowland Bolivian forest: Linking field and remote sensing measurements. *Forest Ecology and Management, 255*(7), 2602–2616.

Brown, S. (1997). Estimating biomass and biomass change of tropical forests: A primer. *FAO Forestry Paper, 134,* Rome, Italy: FAO.

Chambers, J.Q., Asner, G.P., Morton, D.C., Anderson, L.O., Saatchi, S.S., Espírito-Santo, F.D.B., et al. (2007). Regional ecosystem structure and function: Ecological insights from remote sensing of tropical forests. *Trends in Ecology and Evolution, 22*(8), 414–423.

Chave, J., Andalo, C., Brown, S., Cairns, M., Chambers, J.C., Eamus, D., et al. (2005). Tree allometry and improved estimation of carbon stocks and balance in tropical forests. *Oecologia, 145*(1), 87–99.

Chave, J., Riéra, B., & Dubois, M.A. (2001). Estimation of biomass in a neotropical forest of French Guiana: Spatial and temporal variability. *Journal of Tropical Ecology, 17*(1), 79–96.

Claeskens, G., & Hjort, N.L. (2008). *Model selection and model averaging, Vol. 330,* Cambridge: Cambridge University Press.

Clark, D.A., Brown, S., Kicklighter, D.W., Chambers, J.Q., Thomlinson, J.R., & Nif, J. (2001). Measuring net primary production in forests: Concepts and field methods. *Ecological Applications, 11*(2), 356–370.

Clark, D.B., & Clark, D.A. (2000). Landscape-scale variation in forest structure and biomass in a tropical rain forest. *Forest Ecology and Management, 137*(1), 185–198.

Clark, M.L., Roberts, D.A., Ewel, J.J., & Clark, D.B. (2011). Estimation of tropical rain forest aboveground biomass with small-footprint lidar and hyperspectral sensors. *Remote Sensing of Environment, 115*(11), 2931–2942.

Clawges, R., Vierling, K.T., Vierling, L.A., & Rowell, E.M. (2008). The use of lidar remote sensing to estimate avian species diversity, density, and occurrence in a pine/aspen forest. *Remote Sensing of Environment, 112*(5), 2064–2073.

Coops, N.C., Hilker, T., Wulder, M.A., St-Onge, B.A., Newnham, G.J., Siggins, A., & Trofymow, J.A. (2007). Estimating canopy structure of Douglas-fir forest stands from discrete-return LiDAR. *Trees - Structure and Function, 21,* 295–310.

de Liocourt, F. (1898). De l'amanagement des sapinieres. *Bull. Soc. For.* (pp. 396–409) Besancon: Franche-Compte Belfort.

DeFries, R. (2008). Terrestrial vegetation in the coupled human–earth system: Contributions of remote sensing. *Annual Review of Environment and Resources, 33*(1), 369–390.

Denslow, J.S. (1987). Tropical rainforest gaps and tree species diversity. *Annual Review Ecology and Systematics, 18*(1), 431–451.

Drake, J.B., Dubayah, R.O., Clark, D.B., Knox, R.G., Blair, J.B., Hofton, M.A., et al. (2002). Estimation of tropical forest structural characteristics using large-footprint lidar. *Remote Sensing of Environment, 79*(2), 305–319.

Drake, J.B., Dubayah, R., Knox, R., Clark, D., & Blair, J.B. (2002). Sensitivity of large-footprint lidar to canopy structure and biomass in a neotropical rainforest. *Remote Sensing of Environment, 81*(2–3), 378–392.

Drake, J.B., Knox, R.G., Dubayah, R.O., Clark, D.B., Condit, R., Blair, J.B., et al. (2003). Aboveground biomass estimation in closed canopy Neotropical forests using lidar remote sensing: Factors affecting the generality of relationships. *Global Ecology & Biogeography, 12*(2), 147–159.

Dubayah, R., Blair, J.B., Bufton, J.L., Clark, D.B., JaJa, J., Knox, R., et al. (1997). The vegetation canopy LIDAR mission, land satellite information in the next decade II. *American Society for Photogrammetry and Remote Sensing,* 100–112.

Dubayah, R.O., Sheldon, S.L., Clark, D.B., Hofton, M.A., Blair, J.B., Hurtt, G.C., et al. (2010). Estimation of tropical forest height and biomass dynamics using lidar remote sensing at La Selva, Costa Rica. *Journal of Geophysical Research — Biogeosciences, 115.* http://dx.doi.org/10.1029/2009JG000933.

Espírito-Santo, F.D.B., Gloor, M., Keller, M., Malhi, Y., Saatchi, S., Nelson, B., et al. (2014). Size and frequency of natural forest disturbances in Amazonia. *Nature Communications.* http://dx.doi.org/10.1038/ncomms4434.

Feldpausch, T., Banin, L., Phillips, O.L., Baker, T.R., Lewis, S.L., Quesada, C.A., et al. (2010). Height-diameter allometry of tropical trees. *Biogeosciences, 8*(5), 1081–1106.

Frolking, S., Palace, M., Clark, D.B., Chambers, J.Q., Shugart, H.H., & Hurtt, G.C. (2009). Forest disturbance and recovery — A general review in the context of space-borne remote sensing of impacts on aboveground biomass and canopy structure. *Journal of Geophysical Research, 114,* G00E02. http://dx.doi.org/10.1029/2008JG000911.

Garcia, M., Riano, D., Chuvieco, E., & Danson, F.M. (2010). Estimating biomass carbon stocks for a Mediterranean forest in central Spain using lidar height and intensity data. *Remote Sensing of Environment, 114*(4), 816–830.

Gonzalez, P., Asner, G.P., Battles, J.J., Lefsky, M.A., Waring, K.M., & Palace, M. (2010). Forest carbon densities and uncertainties from Lidar, QuickBird, and field inventories in California. *Remote Sensing of Environment, 114*(7), 1561–1575.

Gove, J.H., Ducey, M.J., Leak, W., & Zhang, L. (2008). Rotated sigmoid structures in managed uneven-aged northern hardwood stands: A look at the Burr type III distribution. *Forestry, 81*(2), 161–176.

Gregoire, T.G. (1998). Design-based and model-based inference in survey sampling: Appreciating the difference. *Canadian Journal of Forest Research, 28,* 1429–1447.

Hall, F., Bergen, K., Blair, J.B., Dubayah, R., Emanuel, W., Houghton, R., et al. (2011). Characterizing 3-D vegetation structure from space: Mission capabilities requirements. *Remote Sensing of Environment, 115*(11), 2753–2755.

Hanus, M.L., Hann, D.W., & Marshall, D. (1998). Reconstructing the spatial pattern of trees from routine stand examination measurements. *Forest Science, 44,* 125–133.

Harding, D.J., Lefsky, M.A., Parker, G.G., & Blair, J.B. (2001). Laser altimeter canopy height profiles: Methods and validation for closed-canopy, broadleaf forests. *Remote Sensing of Environment, 76*(3), 283–297.

Hartshorn, G.S. (1980). Neotropical forest dynamics. *Biotropica, 12*(2), 23–30.

Hilker, T., van Leeuwen, M., Coops, N.C., Wulder, M.A., Newnham, G.J., Jupp, D.L.B., et al. (2010). Comparing canopy metrics derived from terrestrial and airborne laser scanning in a Douglas-fir dominated forest stand. *Trees-Structure and Function, 24,* 819–832.

Hilker, T., van Leeuwen, M., Coops, N.C., Wulder, M.A., Newnham, G.J., Jupp, D.L.B., et al. (2014). Comparing canopy metrics derived from terrestrial and airborne laser scanning in a Douglas-fir dominated forest stand. *Trees, 24*(5), 819–832.

Hodgson, M.E., Jensen, J.R., Raber, G., Tullis, J., Davis, B.A., Thompson, G., et al. (2005). An evaluation of lidar-derived elevation and terrain slope in leaf-off conditions. *Photogrammetric Engineering & Remote Sensing, 71*(7), 817–823.

Hodgson, M.E., Jensen, J.R., Schmidt, L., Schill, S., & David, B. (2003). An evaluation of LIDAR- and IFSAR-derived digital elevation models in leaf-on conditions with USGS Level 1 and Level 2 DEMs. *Remote Sensing of Environment, 84*(2), 295–308.

Hofton, M.A., Minster, J.B., & Blair, J.B. (2000). Decomposition of laser altimeter waveforms. *IEEE Transactions on Geoscience and Remote Sensing, 38*(4), 1989–1996.

Hopkinson, C., Lovell, J., Chasmer, L., Jupp, D., Kljun, N., & van Gorsel, E. (2013). Integrating terrestrial and airborne lidar to calibrate a 3D canopy model of effective leaf area index. *Remote Sensing of Environment, 136,* 301–314.

Hunter, M.O., Keller, M., Victoria, D., & Morton, D.C. (2013). Tree height and tropical forest biomass estimation. *Biogeosciences, 10,* 8385–8399. http://dx.doi.org/10.5194/bg-10-8385-2013.

Hurtt, G.C., Dubayah, R., Drake, J., Moorcroft, P., Pacala, S., & Fearon, M. (2004). Beyond potential vegetation: Combining lidar remote sensing and a height-structured ecosystem model for improved estimates of carbon stocks and fluxes. *Ecological Applications, 14*(3), 873–883.

Hurtt, G., Xiao, X., Keller, M., Palace, M., Asner, G.P., Braswell, R., et al. (2003). IKONOS imagery for the large scale biosphere atmosphere experiment in Amazonia (LBA). *Remote Sensing of the Environment, 88*(1–2), 111–127.

Husch, B., Beers, T.W., & Kershaw, J.A., Jr. (2003). *Forest mensuration* (4th ed.). New York: John Wiley & Sons (443 pages).

Jensen, J.R., Humes, K.S., Vierling, L.A., & Hudak, A.T. (2008). Discrete return lidar-based prediction of leaf area index in two conifer forests. *Remote Sensing of Environment, 112,* 3947–3957.

Keller, M., Asner, G.P., Silva, J.M.N., & Palace, M. (2004). Sustainability of selective logging of upland forests in the Brazilian Amazon: Carbon budgets and remote sensing as tools for evaluation of logging effects. In D.J. Zarin, J. Alavalapati, F.E. Putz, & M. Schmink (Eds.), *Working forests in the American tropics: Conservation through sustainable management?.* New York: Publisher, Colombia University Press.

Keller, M., Palace, M., & Hurtt, G. (2001). Biomass estimation in the Tapajos National Forest, Brazil: Examination of sampling and allometric uncertainties. *Forest Ecology and Management, 154*(3), 371–382.

Kellner, J.R., Clark, D.B., & Hubbell, S.P. (2009). Pervasive canopy dynamics produce short-term stability in a tropical rain forest landscape. *Ecology Letters, 12*(2), 155–164.

Lefsky, M.A., Cohen, W.B., Acker, S.A., Parker, G.G., Spies, T.A., & Harding, D. (1999). Lidar remote sensing of the canopy structure and biophysical properties of Douglas-fir western hemlock forests. *Remote Sensing of Environment, 70*(3), 339–361.

Lefsky, M.A., Harding, D.J., Keller, M., Cohen, W.B., Carabajal, C.C., Espirito-Santo, F.D., et al. (2005). Estimates of forest canopy height and aboveground biomass using ICESat. *Geophysical Research Letters, 32*(22), L22S02. http://dx.doi.org/10.1029/2005GL023971.

Lefsky, M.A., Harding, D.J., Keller, M., Cohen, W.B., Carabajal, C.C., Espirito-Santo, F.D., et al. (2006). Correction to "Estimates of forest canopy height and aboveground biomass using ICESat". *Geophysical Research Letters, 32*(5), L05501. http://dx.doi.org/10.1029/2005GL025518.

Lovell, J., Jupp, D.L.B., Culvenor, D.S., & Coops, N.C. (2003). Using airborne and ground-based ranging lidar to measure canopy structure in Australian forests. *Canadian Journal of Remote Sensing, 29*(5), 607–622.

MacArthur, R.H., & Horn, H.S. (1969). Foliage profiles by vertical measurement. *Ecology, 50*(5), 802–804.

MacArthur, R., & MacArthur, J.W. (1961). On bird species diversity. *Ecology, 42*, 594–598.

Mäkelä, A., & Valentine, H.T. (2006). Crown ratio influences allometric scaling in trees. *Ecology, 87*(12), 2967–2972.

Marshall, D.D., Iles, K., & Bell, J.F. (2004). Using a large-angle gauge to select trees for measurement in variable plot sampling. *Canadian Journal of Forest Research, 34*(4), 840–845.

Marthews, T.R., Burslem, D.F.R.P., Phillips, R.T., & Mullins, C.E. (2008). Modelling direct radiation and canopy gap regimes in tropical forests. *Biotropica, 40*(6), 676–685.

Maynard, D.S., Ducey, M.J., Congalton, R.G., & Hartter, J. (2013). Modeling forest canopy structure and density by combining point quadrat sampling and survival analysis. *Forest Science, 59*(6), 681–692 (12).

McDade, L.A., Bawa, K.S., Hespenheide, H.A., & Hartshorn, G.S. (Eds.). (1994). *La Selva: Ecology and natural history of a Neotropical rain forest*. Chicago, Illinois, USA: University of Chicago Press.

McDade, L.A., & Hartshorn, G.S. (1994). La Selva biological station. In L.A. McDade, K.S. Bawa, H.S. Hespenheide, & G.S. Hartshorn (Eds.), *La Selva: Ecology and natural history of a neotropical rain forest* (pp. 6–15). Chicago: The University of Chicago Press.

McGarrigle, E., Kershaw, J.A., Lavigne, M.B., Weiskittel, A.R., & Ducey, M. (2011). Predicting the number of trees in small diameter classes using predictions from a two-parameter Weibull distribution. *Forestry, 84*(4), 431–439.

McMichael, C.H., Bush, M.B., Silman, M.R., Piperno, D.R., Raczka, M., Lobato, L.C., et al. (2013). Historical fire and bamboo dynamics in western Amazonia. *Journal of Biogeography, 40*(2), 299–309.

McMichael, C., Palace, M., Bush, M.B., Braswell, B., Hagen, S.C., Silman, M., et al. (2014). Terra preta distribution in Amazonia. *Proceedings of the Royal Society B.* http://dx.doi.org/10.1098/rspb.2013.2475.

Means, J.E., Acker, S.A., Harding, D.J., Blair, J.B., Lefsky, M.A., Cohen, W.B., et al. (1999). Use of large-footprint scanning airborne lidar to estimate forest stand characteristics in the western Cascades of Oregon. *Remote Sensing of Environment, 67*(3), 298–308.

Meyer, H.A. (1943). Management without rotation. *Journal of Forestry, 41*(2), 126–132.

Meyer, H.A. (1952). Structure, growth, and drain in balanced uneven-aged forests. *Journal of Forestry, 50*(12), 85–92.

Meyer, H.A., & Stevenson, D.D. (1943). The structure and growth of virgin beech-birch-maple-hemlock forests in northern Pennsylvania. *Journal of Agricultural Research, 67*(12), 465–484.

Monsi, M., Uchijima, Z., & Oikawa, T. (1973). Structure of foliage canopies and photosynthesis. *Annual Review of Ecology and Systematics, 4*(1), 301–327.

Montgomery, R.A., & Chazdon, R.L. (2001). Forest structure, canopy architecture, and light transmittance in tropical wet forests. *Ecology, 82*(10), 2707–2718.

Morsdorf, F., Kotz, B., Meier, E., Itten, K.I., & Allgower, B. (2006). Estimation of LAI and fractional cover from small footprint airborne laser scanning data based on gap fraction. *Remote Sensing of Environment, 104*, 50–61.

Morton, D. C., Nagol, J. R., Rosette, J., Carabajal, C. C., Harding, D. J., & Palace, M. W. (2014a). Apparent Seasonal Green up of Amazon Forests. *Nature.* http://dx.doi.org/10.1038/nature13006.

Morton, D.C., Nagol, J.R., Rosette, J., Carabajal, C.C., Harding, D.J., Palace, M.W., et al. (2014b). Seasonal green up of Amazon forests is an infra-red herring. *Nature, 506*(7486).

Nelson, R., Short, A., & Valenti, M. (2004). Measuring biomass and carbon in Delaware using airborne profiling lidar. *Scandinavian Journal of Forest Research, 19*(6), 247–267.

Niinemets, U., & Anten, N.P.R. (2009). Packing the photosynthetic machinery: From leaf to canopy. In A. Laisk, L. Nedbal, & Govindjee (Eds.), *Photosynthesis in silico: Understanding complexity from molecules to ecosystems* (pp. 363–399). Dordrecht: Springer (503 pp.).

Ni-Mester, W., Jupp, D.L., & Dubayah, R. (2001). Modeling Lidar waveforms in heterogeneous and discrete canopies. *IEEE Transactions on Geoscience and Remote Sensing, 39*(9), 1943–1958.

Oderwald, R.G., & Jones, E. (1992). Sample sizes for point, double sampling. *Canadian Journal of Forest Research, 22*(7), 980–983.

Oliver, C.D., & Larson, B.C. (1996). *Forest stand dynamics* (Updated ed.). New York: Wiley, 520.

Ouma, Y.O., Tetuko, J., & Tateishi, R. (2008). Analysis of co-occurrence and discrete wavelet transform textures for differentiation of forest and non-forest vegetation in very-high-resolution optical-sensor imagery. *International Journal of Remote Sensing, 29*(12), 3417–3456.

Palace, M., Keller, M., Asner, G.P., Hagen, S., & Braswell, B. (2008). Amazon forest structure from IKONOS satellite data and the automated characterization of forest canopy properties. *Biotropica, 40*(20), 141–150.

Palace, M., Keller, M., Asner, G.P., Silva, J.N.M., & Passos, C. (2007). Necromass in undisturbed and logged forests in the Brazilian Amazon. *Forest Ecology and Management, 238*, 309–318.

Palace, M., Keller, M., & Silva, H. (2008). Necromass production: Studies in undisturbed and logged Amazon forests. *Ecological Applications, 18*(4), 873–884.

Pekin, B.K., Jung, J., Villanueva-Rivera, L.J., Pijanowski, B.C., & Ahumada, J.A. (2012). Modeling acoustic diversity using soundscape recordings and LIDAR-derived metrics of vertical forest structure in a neotropical rainforest. *Landscape Ecology, 27*(10), 1513–1522.

Popescu, S.C., & Zhao, K. (2008). A voxel-based lidar method for estimating crown base height for deciduous and pine trees. *Remote Sensing of Environment, 112*(3), 767–781.

Rice, A.H., Pyle, E.H., Saleska, S.R., Hutyra, L., Camargo, P.B., Portilho, K., et al. (2004). Carbon balance and vegetation dynamics in an old-growth Amazonian forest. *Ecological Applications, 14*(sp4), s55–s71.

Richards, P.W. (1952). *The tropical rain forest.* Cambridge: Cambridge University Press.

Saatchi, S., Harris, N.L, Brown, S., Lefsky, M., Mitchard, E., Salas, W., et al. (2011). Benchmark map of forest carbon stocks in tropical regions across three continents. *Proceedings of the National Academy of Sciences, 108*(24), 9899–9904.

Schemske, D.W., & Brokaw, N. (1981). Treefalls and the distribution of understory birds in a tropical forest. *Ecology, 62*(4), 938–945.

Shannon, C.E. (1948). A mathematical theory of communication. *The Bell System Technical Journal, 27*, 379–423 (623–656).

Shugart, H.H., Hopkins, M.S., Burgess, I.P., & Mortlock, A.T. (1980). The development of a succession model for subtropical rain forest and its application to assess the effects of timber harvest at Wiangaree State Forest, New South Wales. *Journal of Environmental Management, 11*(3), 243–265.

Spies, T.A. (1998). Forest structure: A key to the ecosystem. In J.A. Trofymow, & A. MacKinnon (Eds.), *Proceedings of a workshop on structure, process, and diversity in successional forests of Coastal British Columbia, February 17–19, 72.* (pp. 34–39). Victoria, British Columbia: Northwest Science (SI No. 2).

Stark, S.C., Leitold, V., Wu, J.L., Hunter, M.O., de Castilho, C.V., Costa, F.R.C., et al. (2012). Amazon forest carbon dynamics predicted by profiles of canopy leaf area and light environment. *Ecology Letters, 15*(12), 1406–1414.

Sullivan, F.B., Palace, M., & Ducey, M.J. (2014). Multivariate statistical analysis of asynchronous lidar data and vegetation models in a neotropical forest. *Remote Sensing of Environment, 154*, 368–377. http://dx.doi.org/10.1016/j.rse.2014.04.027.

Tang, H., Dubayah, R., Swatantran, A., Hofton, M., Sheldon, S., Clark, D.B., et al. (2012). Retrieval of vertical LAI profiles over tropical rain forests using waveform lidar at La Selva, Costa Rica. *Remote Sensing of Environment, 124*, 242–250.

Tansley, A.G. (1935). The use and abuse of vegetational concepts and terms. *Ecology, 16*(3), 284–307.

Terborgh, J. (1985). The vertical component of plant species diversity in temperate and tropical forests. *The American Naturalist, 126*(6), 760–776.

Terrasolid TerraScan (2009). Available online http://www.terrasolid.fi/en.

Treuhaft, R.N., Chapman, B.D., dos Santos, J.R., Goncalves, F.G., Dutra, L.V., Graca, P.M.L.A., et al. (2009). Vegetation profiles in tropical forests from multibaseline interferometric synthetic aperture radar, field, and lidar measurements. *Journal of Geophysical Research, 114*(D23). http://dx.doi.org/10.1029/2008JD011674.

Treuhaft, R.N., Goncalves, F.G., Chapman, B.D., Neumann, M., dos Santos, J.R., de Alencastro, Lima, et al. (2013). Relationships between remotely sensed forest structure and biomass: Fourier structure from Lidar and InSAR and penetration at microwave frequencies. *Revista Brasileira de Cartografia, 65*(4), 747–755.

Treuhaft, R.N., Goncalves, F.G., Drake, J.B., Chapman, B.D., dos Santos, J.R., Dutra, L.V., et al. (2010). Biomass estimation in a tropical wet forest using Fourier transforms of profiles from lidar or interferometric SAR. *Geophysical Research Letters, 37*(23). http://dx.doi.org/10.1029/2010GL045608.

Treuhaft, R., Gonçalves, F., Roberto dos Santos, J., Keller, M., Palace Palace, M., Madsen, S., et al. (2015). Tropical-forest biomass estimation at X-band from the spaceborne TanDEM-X interferometer. *IEEE Geoscience and Remote Sensing Letters, 12*(2), 239–243.

Tropical Ecology Assessment & Monitoring (TEAM) Network of Conservation International (2009). *Small-footprint, discrete return lidar dataset collected over La Selva by Northrop Grumman Corporation through the Global Climate Monitoring Systems and 3001 remote sensing division.*

Unger, M., Homeier, J., & Leuschner, C. (2013). Relationships among leaf area index, below-canopy light availability and tree diversity along a transect from tropical lowland to montane forests in NE Ecuador. *Tropical Ecology, 54*(1), 33–45.

Vierling, L.A., Rowell, E., Chen, X., Dykstra, D., & Vierling, K. (2002). Relationships among airborne scanning lidar, high resolution multispectral imagery, and ground-based inventory data in a ponderosa pine forest. *Geoscience and Remote Sensing Symposium, 2002. IGARSS'02. 2002 IEEE International (vol. 5) Toronto, Canada.*

Vitousek, P.M., & Denslow, J.S. (1986). Nitrogen and phosphorus availability in treefall gaps of a lowland tropical rainforests. *Journal of Ecology, 74*(4), 1167–1178.

Weishampel, J.F., Drake, J.B., Cooper, A., Blair, J.B., & Hofton, M. (2007). Forest canopy recovery from the 1938 hurricane and subsequent salvage damage measured with airborne lidar. *Remote Sensing of Environment, 109*(2), 142–153.

Whitmore, T.C. (1982). On pattern and process in forests. In E.I. Newman (Ed.), *The plant community as a working mechanism* (pp. 45–59). Oxford: Blackwell Scientific Publications.

Zhao, K., Popescu, S., & Nelson, R. (2009). Lidar remote sensing of forest biomass: A scale-invariant estimation approach using airborne lasers. *Remote Sensing of Environment, 113*(1), 182–196.